Polymer Chemistry
RSCPublishing

ARTICLE

Microstructure and Melt Properties of CO-Ethylene Copolymers with Remarkably Low CO-Content

Cite this: DOI: 10.1039/x0xx00000x

Saeeda S. Soomro,[a] Daniela Cozzula,[a] Walter Leitner,[b] Henning Vogt [a] and Thomas E. Müller [a]*

Received 00th January 2012,
Accepted 00th January 2012

DOI: 10.1039/x0xx00000x

www.rsc.org/

Polymer Chemistry RSCPublishing

ARTICLE

Supplementary information

Materials

Palladium acetate (99 %) and deuterated chlorobenzene (99 %) were obtained from Sigma-Aldrich. The parent protonated phosphine sulphonato ligand **HL** was purchased from Convertex®. Ethylene (3.0) was obtained from Gerling Holz & Co. Hamburg; carbon monoxide (3.7) was acquired from Praxair, Belgium. Dichloromethane was distilled over CaH_2 and degassed by the freeze-pump-thaw technique.

Synthesis of polyketones

Reaction conditions for the synthesis of polyketones **P1** to **P11** by copolymerization of carbon monoxide and ethylene are summarised in Table S1.

Table S1. Reaction conditions and yield in the Pd-catalysed copolymerization of CO and ethylene to polyketones **P1** to **P11** and reference samples **R1** and **R2**.

Poly-ketone	c(Pd) [a] [10^{-3} mol·l^{-1}]	Ratio CO/C_2H_4	T [ºC]	Time [h]	TOF [g·(mmol$_{Pd}$·h)$^{-1}$]	Yield [g]
R1	0.1 [b]	20/20	115	17	-	2.2
P1	0.05	15/35	110	18	17	15
P2	0.05	12/38	110	18	13	12
P3*	0.05	6/44	110	17	11	9.2
P4	0.05	1/49	110	2.5	96	12
P5	0.05	1/49	110	6.5	102	33
P6	0.037	1/49	110	2.0	75	5.6
P7	0.025	1/49	110	2.5	53	3.3
P8	0.01	1/49	110	60	10	0.6
P9	0.05	1/49	100	3.0	66	9.9
P10	0.05	1/49	120	2.5	76	9.5
P11	0.05	1/49	130	2.0	100	10
R2	0.02	1/49	110	1.0	-	15
PE	0.015	0/50	110	1.6	-	4.2

[a] Ratio $Pd(OAc)_2$/HL 1/1.5; [b] Ligand **HL** replaced with DPPPr = *bis*-diphenylphosphinopropane.

More detailed investigation of the gas uptake with time during the preparation of the polyketones **P1-P11** showed that the reaction proceeded in three distinct phases. After an induction period (t_{ind}) of 10 min where hardly any gas consumption occurred, gas uptake commenced slowly for about 40 min (initiation period t_{ini}, **P4**: 11×10^{-3} $g_{CO/C2H4}$/min). Thereafter, the reaction accelerated, and the gas uptake became faster (**P4**: 107×10^{-3} $g_{CO/C2H4}$/min). The rate of the gas uptake was approximately constant for the remaining reaction time.

Methods used for characterization of the polyketones

^{1}H and ^{13}C{^{1}H} NMR spectra were measured on a Bruker, AV III 300 NMR spectrometer in deuterated chlorobenzene at 95 °C (**P2-P11, R2**) or 1,1,1,3,3,3-hexafluoroisopropanol (HFIP)/C_6D_6 at room temperature (**P1**, **R1**). The CO content was determined from the ^{1}H NMR spectra as described in the literature.[1]

The molecular weight distribution was determined by high-temperature GPC analysis. The analyses were performed at 150°C on a PSS Polefin 10 µm, 1000 Å, ID 8.0 mm x 300 mm column against polystyrene as standard. The eluting solvent was 1,2,4-trichlorobenzene (flow rate 1.0 mL/min).

The phase behaviour was characterized on a Perkin-Elmer Pyris 6 differential scanning calorimeter. A sample of the polymer (*ca*. 10 mg, **R1**, **P4-P11, R2**, **PE**) was placed into the sample holder. The latter was placed into a flow of argon, and the temperature was adjusted to 25°C. Then, the sample was heated at 10 °C min^{-1} to a temperature at least 50°C below T_d, cooled to 25°C (10°C min^{-1}) and held there for 2 min. The heating and cooling cycle was repeated. For the polymers **P2** and **P3,** the temperature was adjusted initially to -50°C. Then, the sample was heated to 220 °C at 10 °C min^{-1}, cooled to -50°C (10°C min^{-1}) and held there for 5 min. The heating and cooling cycle was repeated. The melting point and the solidification temperature are given as the minimum/maximum of the heat flow curve in the second heating/cooling cycle.

The crystallinity of polymer samples was calculated by Equation 1a-c, whereby H' is the heat given off by that part of the polymer which was crystalline before heating, H_m the heat of melting, H_c the heat of cooling, H^*_m the specific heat of melting, m_c the amount of polymer that was crystalline, m the weight of the sample, χ the crystallinity in percent.

$$\boldsymbol{H' = H_m - H_c}$$

$$\boldsymbol{m_c = \frac{H'}{H^*_m}}$$

$$\chi = \frac{\boldsymbol{m_c}}{\boldsymbol{m}} \times \mathbf{100}\%$$

Equation 1a-c. Calculation of the crystallinity from the difference between the heat of melting and the heat of solidification.

The melting points were confirmed by heating a sample of the polymer (*ca*. 2 mg) on a melting point meter (Schorpp Gerätetechnik MPM-HV2) following the transparency of the sample.

The viscosity of the polymers (**P4-P11**, **R2**) was determined on a Physica MCR 501 Rheometer from Anton Paar using a cone-plate geometry (measuring system DCP35). The sample (0.1 g) was applied to the rheometer plate, heated to 160 °C and subjected to a shear rate increasing from 0.01 to 1000 s^{-1} within 10 min. The viscosity is given as the average viscosity in the range of 200 to 770 s^{-1}. Samples **R1**, **P1**, **P2**, **P3** and **PE** did not melt.

Thermogravimetric analysis (TGA) traces were recorded on a Mettler Toledo Gas Controller GC20 with STRe System. A sample of the polymer (*ca*. 20 mg) was placed into a flow of argon and the temperature adjusted to 25°C. The sample was then heated to 600°C at 10°C · min^{-1} and the weight loss recorded.

Powder XRD patterns were collected on a Stoe STADI P powder diffractometer (STOE & Cie KG, Darmstadt; transmission mode) equipped with a Johann Germanium monochromator (Cu-K$_{\alpha}$1 radiation) and an image plate detector. A sample of the polymer was placed on a flat sample holder and the XRD pattern recorded in the range of $0° \leq 2\Theta \leq 130°$ in 0.015° steps. The program WinXPOW was used to fit the profiles.

Characterization of polyketones

The IR spectra of polyketones **P1** – **P11** in comparison to the spectra of reference samples **R1**, **R2** and **PE** are shown in Figure S1.

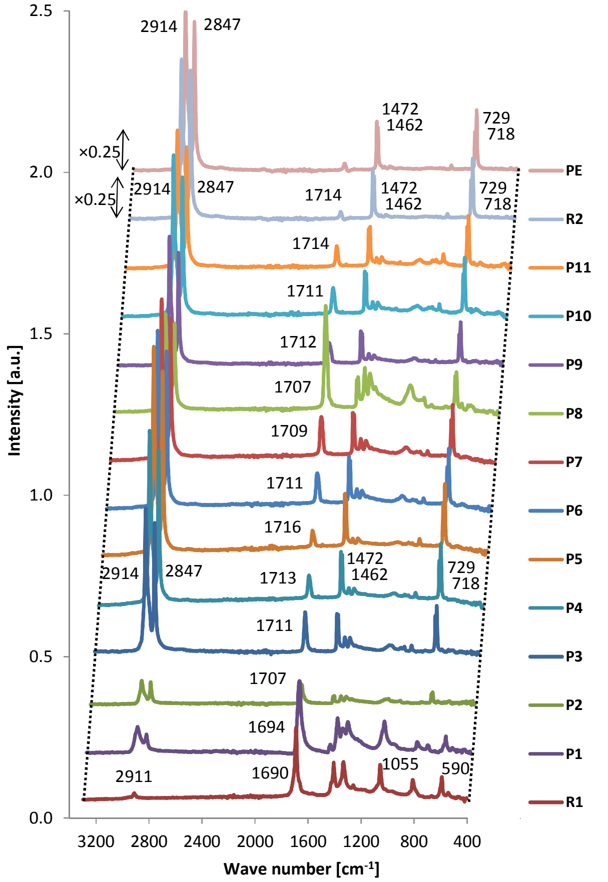

Figure S1. IR spectra of polyketones **P1** – **P11** compared to those of polyketone **R1** with alternating CO-C_2H_4 segments, reference material **R2** with very low CO content and polyethylene **PE**.

The contribution of moieties α, β and γ to the CO stretch vibration in the IR spectra of polyketones **P1** – **P11** and reference samples **R1**, **R2** and **PE** was analysed by deconvolution of the signal in the range of 1800 – 1600 cm^{-1} based on the assumption that the extinction coefficient of the carbonyl band in each moiety is equal (Figure S2 - Figure S14).

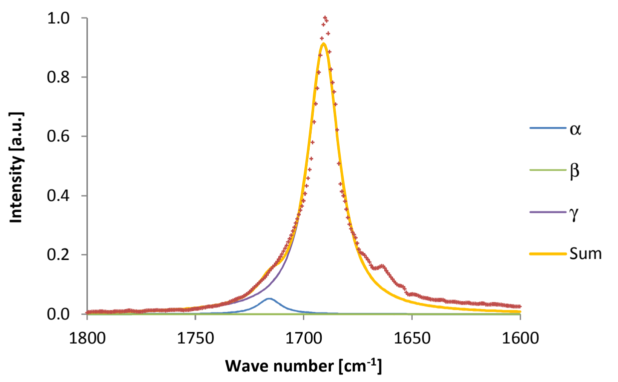

Figure S2. Deconvolution of the CO stretch vibration in the IR spectrum of **R1**.

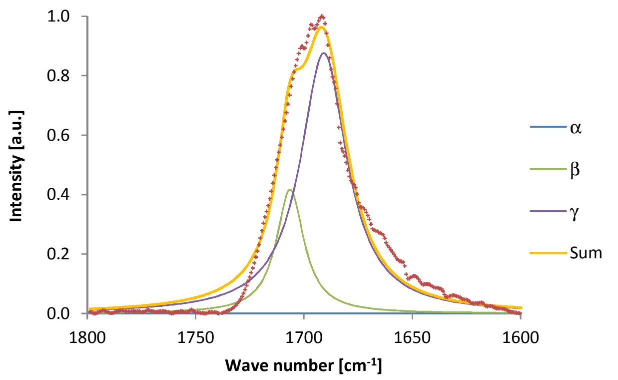

Figure S3. Deconvolution of the CO stretch vibration in the IR spectrum of **P1**.

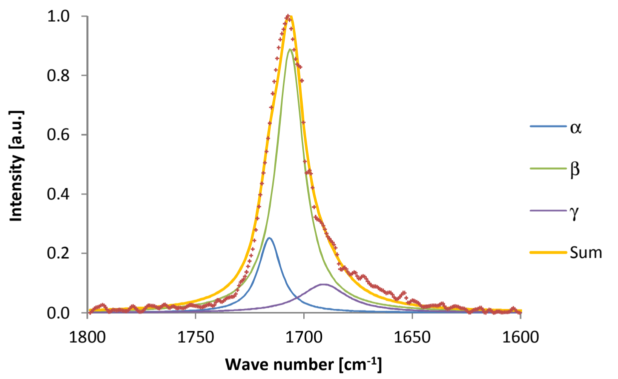

Figure S4. Deconvolution of the CO stretch vibration in the IR spectrum of **P2**.

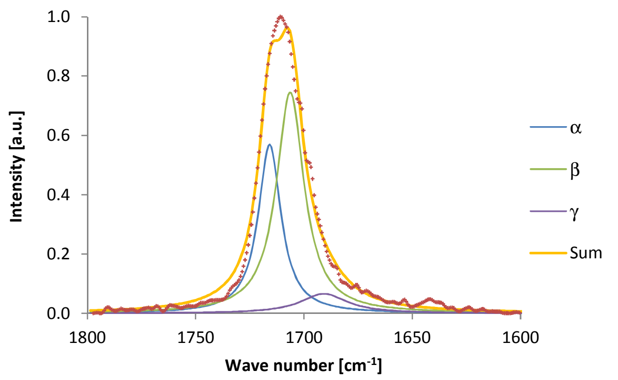

Figure S5. Deconvolution of the CO stretch vibration in the IR spectrum of **P3**.

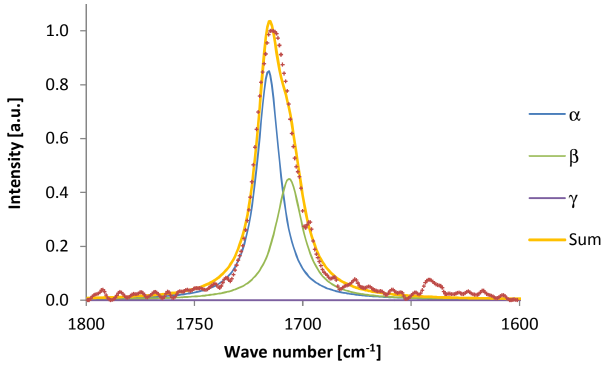

Figure S6. Deconvolution of the CO stretch vibration in the IR spectrum of **P4**.

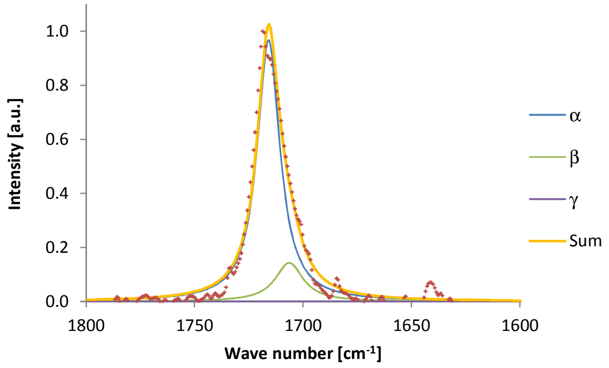

Figure S7. Deconvolution of the CO stretch vibration in the IR spectrum of **P5**.

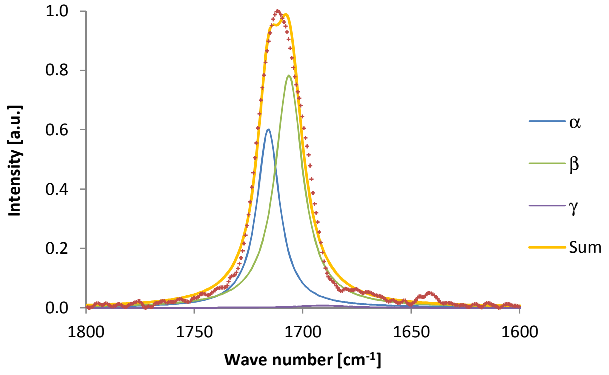

Figure S8. Deconvolution of the CO stretch vibration in the IR spectrum of **P6**.

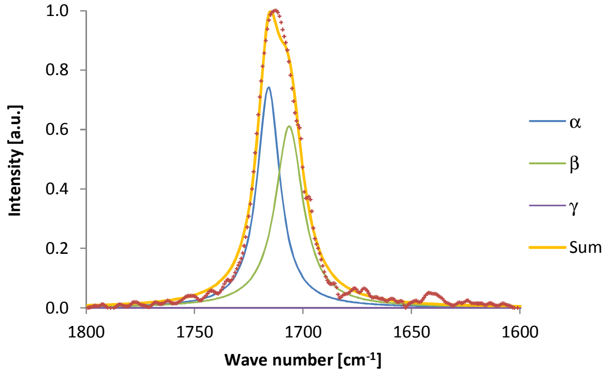

Figure S9. Deconvolution of the CO stretch vibration in the IR spectrum of **P7**.

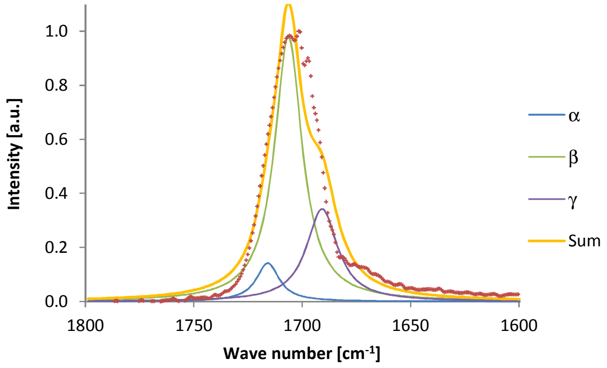

Figure S10. Deconvolution of the CO stretch vibration in the IR spectrum of **P8**. Note that the position ν_i of the contributions of moieties α, β and γ were refined to a common position for polyketones **P1** – **P11** and reference samples **R1** and **R2** giving rise to the less accurate fit in the case of polyketone **P8**.

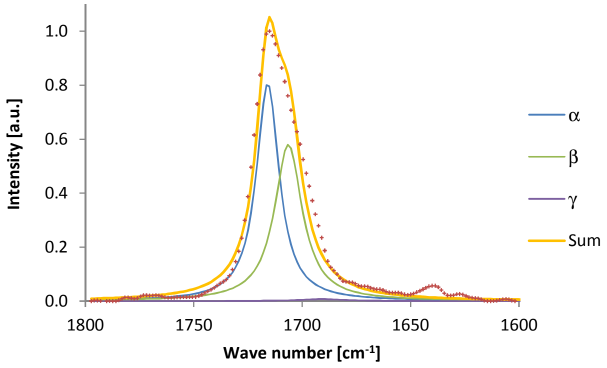

Figure S11. Deconvolution of the CO stretch vibration in the IR spectrum of **P9**.

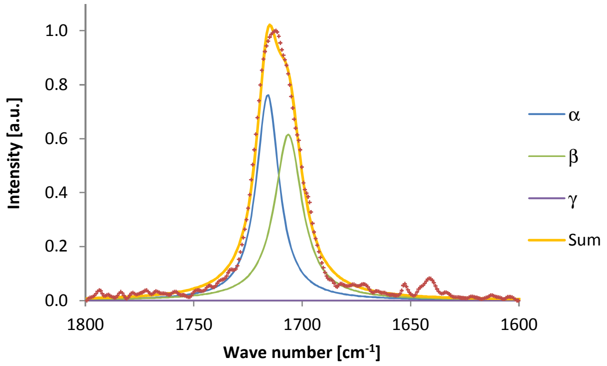

Figure S12. Deconvolution of the CO stretch vibration in the IR spectrum of **P10**.

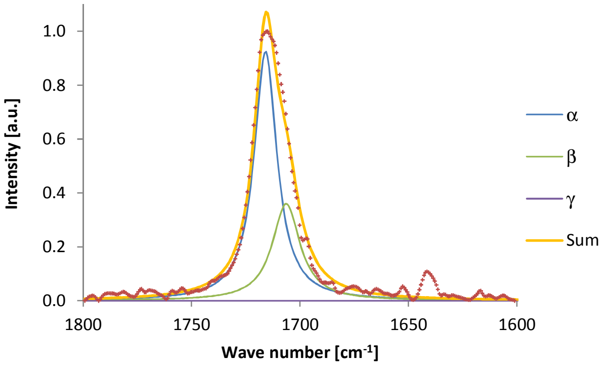

Figure S13. Deconvolution of the CO stretch vibration in the IR spectrum of **P11**.

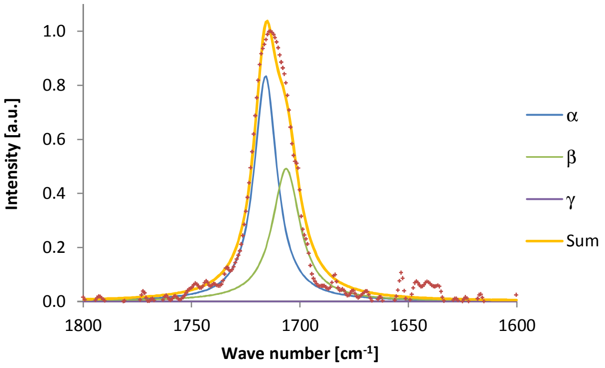

Figure S14. Deconvolution of the CO stretch vibration in the IR spectrum of **R2**.

The contribution of moieties α, β and γ to the CO stretch vibration in the IR spectra of polyketones **P1** – **P11** and reference samples **R1**, **R2** and **PE** was obtained by deconvolution of the signal in the range of 1800 – 1600 cm^{-1} (Table S2).

Table S2. Position of the CO stretch vibration and relative intensity of moieties α, β and γ in polyketones **P1** to **P11** in comparison to reference samples **R1** and **R2**.

Poly-ketone	CO content [wt%]	$\upsilon_{C=O}$ [a] [cm^{-1}]	Moiety α	β	γ
R1	50.0	1690	0.04	0.00	0.96
P1	28.9	1694	0.00	0.22	0.78
P2	16.1	1707	0.16	0.71	0.13
P3*	3.7	1712	0.35	0.56	0.08
P4	2.5	1713	0.61	0.39	0.00
P5	1.5	1716	0.85	0.15	0.00
P6	2.4	1710	0.38	0.61	0.01
P7	5.5	1709	0.50	0.50	0.00
P8	13.5	1707 [b]	0.08	0.66	0.26
P9	2.4	1712	0.53	0.46	0.01
P10	3.0	1711	0.50	0.50	0.00
P11	2.4	1714	0.68	0.32	0.00
R2	0.7	1714	0.58	0.42	0.00

[a] Maximum of the $\upsilon_{C=O}$ vibration; [b] Three distinct maxima at 1713, 1702 and 1693 cm^{-1}.

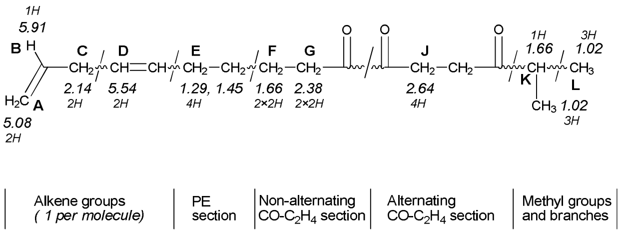

Scheme S1. Assignment of the signals in the ^1H NMR spectrum of polyketone **P4**.

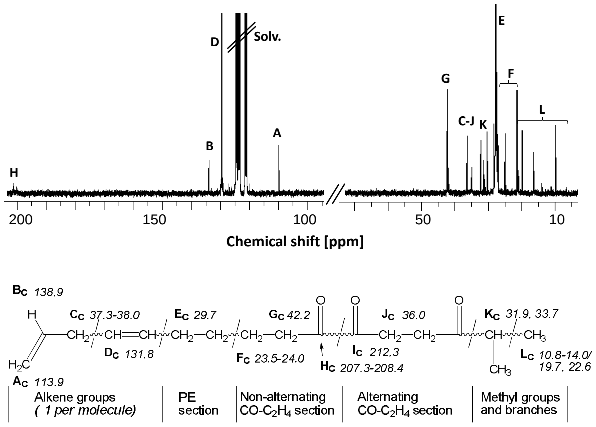

Figure S15. Selected range of the $^{13}C\{^1H\}$ NMR spectrum of **P2** (top) and assignment of the signals (bottom).

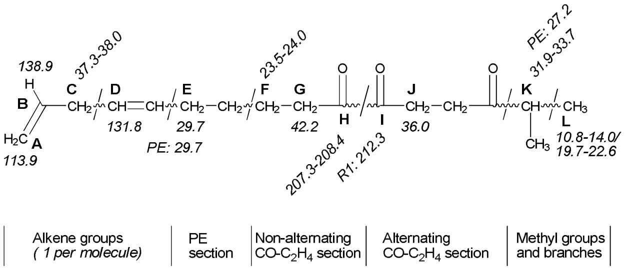

Scheme S2. Range for the signals observed in the $^{13}C\{^1H\}$ NMR spectra of polyketones **P1**-**P11**.

The molecular features of the polyketones were quantified by analysis of the integrals of the ^1H NMR spectra according to Equation S2 to Equation S5.

$$M_n = \frac{(A+B+C+D+E+F+2G+2J+K+L)\times\frac{28}{4}}{\frac{D}{2}+\frac{A+B}{3}}$$

Equation S2. Calculation of the molecular weight based on the integrals of the signals in the ^1H NMR spectra.

$$\frac{n_b}{n_{C2H4}} = \frac{\frac{L}{3}-\frac{A+B}{3}-\frac{D}{2}}{A+B+C+D+E+F+G+J+K+L}$$

Equation S3. Calculation of the average number of branches n_b per ethylene unit based on the integrals of the signals in the ^1H NMR spectra.

$$\boldsymbol{n_l} = \frac{(\boldsymbol{A}+\boldsymbol{B}+\boldsymbol{C}+\boldsymbol{D}+\boldsymbol{E}+\boldsymbol{F}+\boldsymbol{G}+\boldsymbol{K}+\boldsymbol{L})\times 2}{\boldsymbol{G}}$$

Equation S4. Calculation of the average length n_l of the oligomeric $-(C_2H_4)_n-$ segments between two neighbouring CO groups in non-alternating segments based on the integrals of the signals in the ^{1}H NMR spectra.

$$\boldsymbol{n_{CH2\ alt}} = \frac{\boldsymbol{F}}{(\boldsymbol{A}+\boldsymbol{B}+\boldsymbol{C}+\boldsymbol{D}+\boldsymbol{E}+\boldsymbol{F}+\boldsymbol{G}+\boldsymbol{J}+\boldsymbol{K}+\boldsymbol{L})}$$

Equation S5. Calculation of CH_2 groups neighbouring isolated and non-alternating CO-C_2H_4 (α+β moieties) based on the integrals of the signals in the ^{1}H NMR spectra.

The structural data of the polyketones are summarised in Table S3.

Table S3. Structural data for polyketones **P1** to **P11**.

Poly-ketone	CO content [wt%]	Isolated CO groups [wt%]	PE content [wt%]	Segment length [a] [units]	No. of branches [%] [b]
P1	28.9	13.9	42.2	8.1	1.54
P2	16.1	12.3	67.7	13.0	0.24
P3	3.7	2.9	92.6	66.2	0.59
P4	2.5	1.8	95.1	107.2	0.20
P5	1.5	1.2	97.0	159.3	0.17
P6	2.4	1.8	95.2	105.1	0.28
P7	5.5	3.4	88.9	54.6	0.27
P8	13.5	9.7	73.1	17.1	0.06
P9	2.4	1.8	95.3	105.0	0.18
P10	3.0	2.1	94.0	91.6	0.25
P11	2.4	1.9	95.2	103.8	0.41

[a] Average segment length between two neighbouring CO groups in moieties γ; [b] Average number of methyl groups per ethylene unit.

The molecular weight of the polyketones was calculated from an end group analysis based on the ^{1}H NMR data (Table S4)

Table S4. Position of the CO stretch vibration and relative intensity of moieties α, β and γ in polyketones **P1** to **P11** in comparison to reference samples **R1** and **R2**.

Poly-ketone	CO content [wt%]	M_n [g·mol] [a]	PDI [-] [b]
R1	50.0	-	-
P1	28.9	-	-
P2	16.1	3077	2.3
P3*	3.7	2843	1.9
P4	2.5	5272	1.7
P5	1.5	3919	2.1
P6	2.4	5413	1.8
P7	5.5	5827	1.7
P8	13.5	5408	2.0
P9	2.4	5610	2.1
P10	3.0	3580	2.2
P11	2.4	2539	2.1
R2	0.7	5811	-

[a] Determined by ^{1}H NMR spectroscopy, soluble fraction; [b] Determined by GPC chromatography.

By using gel permeation chromatography, the polydispersity of polyketones **P2**-**P11** in dependence of the reaction conditions, *i.e.*, the CO/C_2H_4 ratio employed (Figure S16), the amount of CO/C_2H_4 gas mixture consumed (Figure S17), the catalyst loading (Figure S18) and the reaction temperature (Figure S19) was determined (Table S4). Note that the molecular weight in gel permeation chromatography was referenced to polystyrene standard.

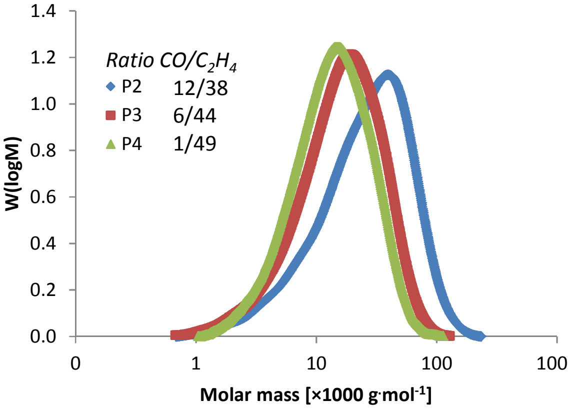

Figure S16. Overlay of the GPC curves of non-alternating polyketones which were obtained by varying the CO/C_2H_4 ratio (**P1**-**P4**).

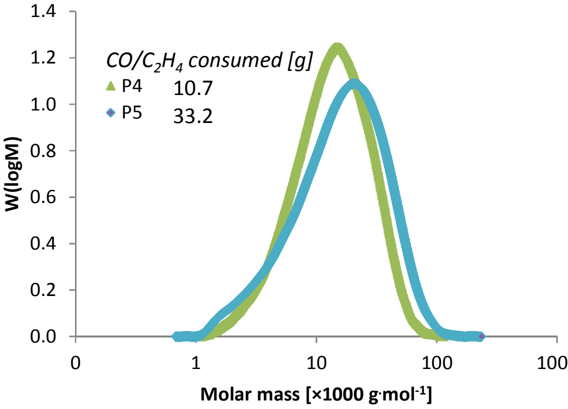

Figure S17. Overlay of the GPC curves of non-alternating polyketones which were obtained after a different amount of CO/C_2H_4 gas mixture had been consumed (**P4**-**P5**).

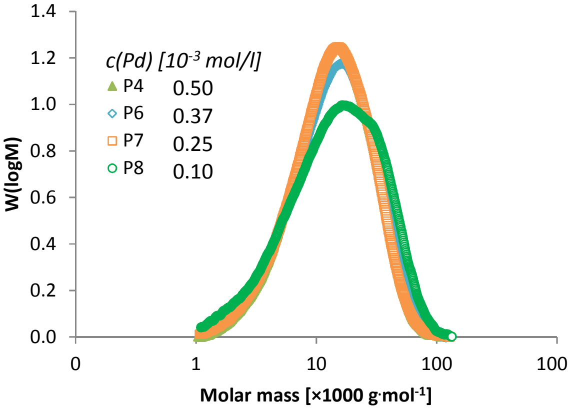

Figure S18. Overlay of the GPC curves of non-alternating polyketones which were obtained by varying the catalyst loading (**P4**, **P6**-**P8**).

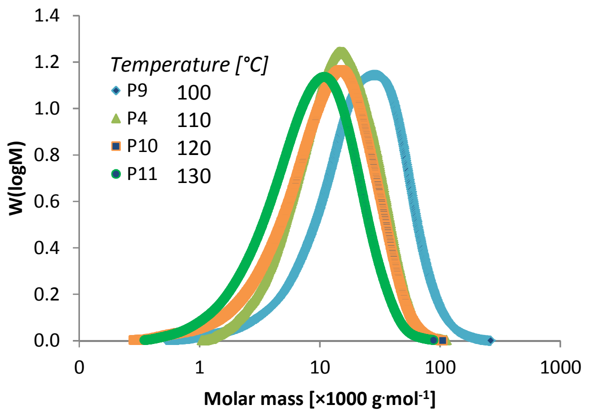

Figure S19. Overlay of the GPC curves of non-alternating polyketones which were obtained by varying the temperature (**P4**, **P9**-**P11**).

The phase transitions of polyketones **P1** – **P11** and of reference samples **R1**, **R2** and **PE** were followed by differential scanning calorimetry (DSC). The DSC traces observed for **P4** are shown in Figure S20.

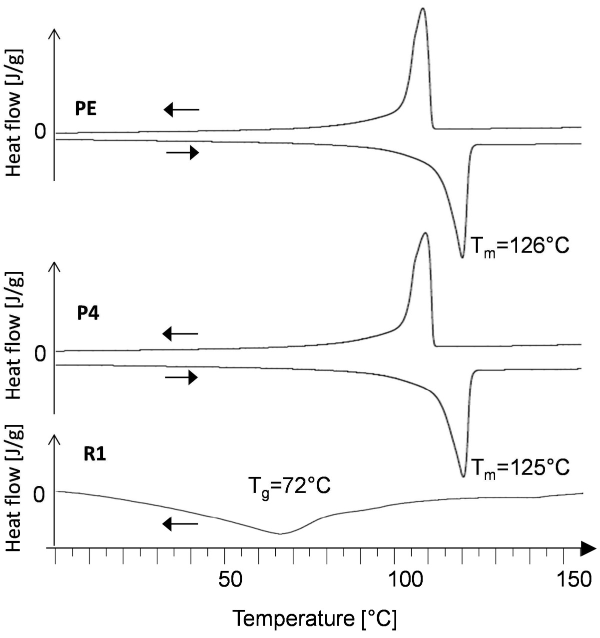

Figure S20. DSC traces observed upon heating and cooling of **P4** (middle) in comparison to **PE** (top) and **R1** (bottom) as reference samples.

The melting points of polyketones **P1** – **P11** and of reference samples **R1**, **R2** and **PE** were confirmed by melting the samples on a melting point meter optically following the transparency of the samples (Table S5). Also reported is the crystalline fraction as derived from analysis of the differences between melting and solidification enthalpy.

Table S5. Physicochemical and intrinsic properties of polyketones **P1** to **P11** compared to those of reference samples **R1** and **R2**.

Polyketone	CO content [wt%]	T_m [a] [°C] [a]	Crystallinity [b] [%]	Domain size [c] [nm]
R1	50.0	>220	-	11.5 (4.2)
P1	28.9	>220	-	9.5 (2.8)
P2	16.1	>220	8.5	17.9 (9.0)
P3	3.7	≈220	7.4	27.2 (2.2)
P4	2.5	127.1	17	20.3 (5.5)
P5	1.5	125.9	20	19.0 (4.4)
P6	2.4	125.7	47	19.1 (5.4)
P7	5.5	123.3	22	19.0 (3.7)
P8	13.5	125.1	17	14.2 (5.3)
P9	2.4	126.9	18	17.7 (6.7)
P10	3.0	121.2	17	18.1 (6.7)
P11	2.4	122.0	12	19.8 (5.6)
R2	0.7	128.6	2	16.2 (4.5)
PE	---	128.3	13	27.8 (5.8)

[a] Determined on melting point meter; [b] Determined by calorimetry; [c] From analysis of the peak width in powder XRD powder pattern.

When polyketones without alternating segments (**P4-P7**, **P9-P11**) were heated in a stream of inert gas, the onset temperature of a weight loss (T_d) was observed in the range of 464-469°C; decomposition was associated with a weight loss of 93-98% (Table S6).

Table S6. Onset temperature T_d of thermal degradation of polyketones **P1-P11** in comparison to reference samples **R1**, **R2** and **PE**.

Polyketone	T_d [°C]	Weight loss [%]	T_d [°C]	Weight loss [%]
	Step 1	*Step 1*	*Step 2*	*Step 2*
R1	339.1	58.0	- [a]	- [a]
P1	244.9	13.2	395.4	53.9
P2	233.0	8.1	430.8	74.8
P3*	223.4	3.5	450.6	83.3
P4	-	-	468.7	95.6
P5	-	-	464.0	96.9
P6	-	-	468.0	95.3
P7	-	-	466.9	93.1
P8	215.8	3.1	451.7	87.5
P9	-	-	464.8	96.4
P10	-	-	469.1	95.1
P11	-	-	466.7	96.1
R2	-	-	463.6	98.0
PE	-	-	468.0	99.6

[a] No further weight loss until 600°C.

The powder XRD diffractograms of the polyketones are given in Figure S21. **P4** gave rise to a strong reflection at 23.88° and a series of weaker reflections at 29.99, 36.24, 39.77, 40.67, 41.64, 42.91, 43.90, 46.84, 52.91 and 54.84°. All other samples (**P5** to **R2**) exhibited the same set of signals as **P4** but varied in intensity. Comparison with the powder diffractogram of **PE** showed that these reflections are characteristic for domains of polycrystalline polyethylene. Analysing the half width of the most relevant reflections, an average domain size of 18.2(3.7) nm was estimated (Table S5).

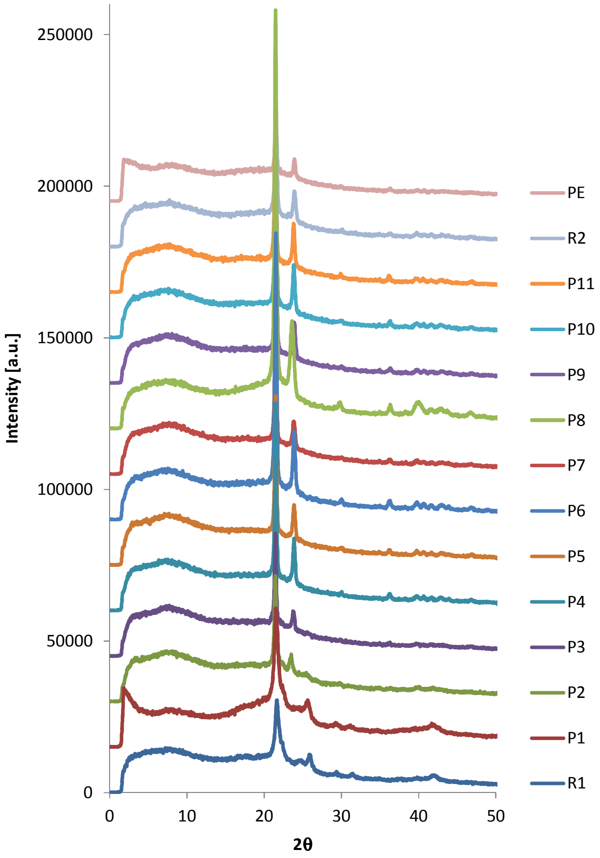

Figure S21. Diffraction patterns of polyketones **P1** – **P11** compared to those of polyketone **R1** with alternating CO-C_2H_4 segments, reference material **R2** with very low CO content and polyethylene **PE**.

References

1. R. Luo, D. K. Newsham and A. Sen, *Organometallics*, 2009, **28**, 6994-7000.